AIAA JOURNAL
Vol. 36, No. 11, November 1998

Forward and Inverse Analysis for Impact on Sandwich Panels

Cheng-Zorn Tsai,* Enboa Wu,† and Bin-Horn Luo‡
National Taiwan University, Taipei, Taiwan 106, Republic of China

A Green's function approach is presented for forward and inverse analyses of sandwich panels that were struck transversely at low velocities. To model the dynamic response of the panel, both membrane and bending deformations of the laminated face plates were considered, and the core, in this case made of honeycomb, was treated to deform by transverse shear force. The displacement field of the panel as a whole was then modeled using beam functions along with the Rayleigh–Ritz method. The derived coupled equations of motion were further transferred to the eigenspace to form Green's function. In the forward analysis, the solution was obtained directly, and the agreement between the prediction and the measured data was found to be very satisfactory when the impact location was beyond a distance that was a few times the panel thickness. On the other hand, a constrained optimization method was employed in the inverse analysis to search for the optimal impact force history from the recorded strain histories. The determined force history was also found to have a very satisfactory agreement with the measured one.

Introduction

BECAUSE of their low weight and high flexural stiffness, sandwich panels have been used extensively in the aeronautical industry. In the early years, studies mainly focused on static and vibration analyses of these advanced structures. In 1948, Reissner[1] proposed a model that included membrane deformation but neglected the bending deformation in modeling the face plate of a sandwich panel. A refined model was soon proposed by Hoff and Mautner[2] to include both the membrane and bending effect in the face plate. Comprehensive investigations on the bending stiffness and stability of sandwich panels were carried out by Plantema[3] and Allen.[4] In a series of papers, Yu[5–8] performed detailed analyses on the vibration responses of sandwich panels, in which the face plates and the core were considered to deform linearly. This work was later extended by other researchers.[9–11] On the vibration analysis of sandwich panels with variable thickness, Chang and Chen[12] employed the Mindlin plate theory to model the response of the face plates.

On the other hand, fewer results have been reported on the low-velocity impact response of sandwich panels. A preliminary result was presented by Sun and Wu,[13] who performed finite element analyses on sandwich panels. The modified Hertz contact law was employed to relate the indentor movement to the displacement history of the panel, and failure mechanisms were identified. A more complete impact analysis on sandwich panels, in which the core was made of elastic foam, was presented by Lee et al.[14] In this analysis, the Mindlin plate theory was employed to model the response of the face plates, and the core was assumed to deform linearly. Recently, a complete review of impact on sandwich structures was performed by Abrate.[15]

Even fewer results have appeared for impact responses of honeycomb-cored sandwich panels. In 1992, Goldsmith and Sackman[16] studied the energy absorption capability of honeycomb sandwich panels, in which the face plates were made of aluminum. The impact behavior of a sandwich beam was investigated in a three-point bending configuration by Mines et al.[17] Additionally, a complete investigation of static and dynamic responses of six types of honeycombs was recently reported by Wu and Jiang.[18] In this study, a significant loading rate effect was uncovered.

Received Oct. 24, 1997; revision received June 25, 1998; accepted for publication June 29, 1998.

*Postdoctoral Research Associate, Institute of Applied Mechanics.
†Professor, Institute of Applied Mechanics. E-mail: ebwu@spring.iam.ntu.edu.tw.
‡Graduate Student, Institute of Applied Mechanics.

The goal of the present study was to develop a Green's function method for both forward and inverse analyses of a sandwich panel subjected to low-velocity impact. A system of equations of motion will first be built using a simple expression of the displacement field for the core and the face plates. These coupled equations will be transferred to the eigenspace of the model so that the equations are all decoupled and are then expressed in a form of Green's function. The forward solution will then be obtained directly. On the other hand, a constrained optimization method will be employed in the inverse analysis to search for the optimal impact force history from the recorded responses of the panel. This time-domain method is different from the frequency-domain method developed by Martin and Doyle[19] and Doyle.[20] The results of both forward and inverse analyses will then be compared with the experimental data to validate the developed Green's function method, the proposed mathematical model, and the solution procedure.

Governing Equations

As shown in Fig. 1, both membrane and bending deformations are considered to model the displacement field of the face plates. The mathematical forms for the upper and lower face plates are expressed as

$$u^{\pm}(x, y, z, t) = \mp\frac{1}{2}(h + t_f)\psi_x - \left(z \mp \frac{h + t_f}{2}\right)\frac{\partial w}{\partial x}$$

$$v^{\pm}(x, y, z, t) = \mp\frac{1}{2}(h + t_f)\psi_y - \left(z \mp \frac{h + t_f}{2}\right)\frac{\partial w}{\partial y} \qquad (1)$$

$$w^{\pm}(x, y, z, t) = w$$

where the + and − signs on the left-hand side of Eq. (1) are for the upper and lower face plates, respectively.

The displacement of the core is

$$u_c(x, y, z, t) = -z\left(\frac{h + t_f}{h}\psi_x - \frac{t_f}{h}\frac{\partial w}{\partial x}\right)$$

$$v_c(x, y, z, t) = -z\left(\frac{h + t_f}{h}\psi_y - \frac{t_f}{h}\frac{\partial w}{\partial y}\right) \qquad (2)$$

$$w_c(x, y, z, t) = w$$

where w is the transverse displacement of the face plates; ψ_x and ψ_y are rotations of the z plane of the core in the x and y directions, respectively; h is the thickness of the core; and t_f is the thickness of the face plate. Thus, only the transverse shear deformation of the core is considered in Eq. (2).

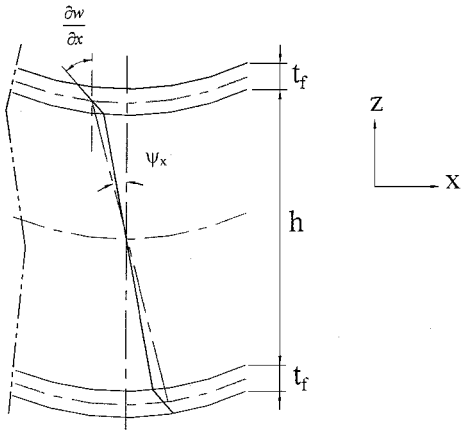

Fig. 1 Displacement field of a sandwich panel.

The strain vs displacement relationships for the face plates and the core can be obtained by direct differentiation of Eqs. (1) and (2). The explicit form for the face plates is

$$\epsilon_{xx}^{\pm}(x,y,z,t) = \mp\frac{1}{2}(h+t_f)\psi_{x,x} - \left(z \mp \frac{h+t_f}{2}\right)\frac{\partial^2 w}{\partial x^2}$$

$$\epsilon_{yy}^{\pm}(x,y,z,t) = \mp\frac{1}{2}(h+t_f)\psi_{y,y} - \left(z \mp \frac{h+t_f}{2}\right)\frac{\partial^2 w}{\partial y^2} \tag{3}$$

$$\gamma_{xy}^{\pm}(x,y,z,t) = \mp\frac{1}{2}(h+t_f)[\psi_{x,y}+\psi_{y,x}] - 2\left(z \mp \frac{h+t_f}{2}\frac{\partial^2 w}{\partial x \partial y}\right)$$

The shear strains of the core are

$$\gamma_{xz}^{c}(x,y,z,t) = [(h+t_f)/h](w_{,x} - \psi_x)$$
$$\gamma_{yz}^{c}(x,y,z,t) = [(h+t_f)/h](w_{,y} - \psi_y) \tag{4}$$

The constitutive relationship for the face plate and the core are

$$\begin{pmatrix}\sigma_{xx}\\ \sigma_{yy}\\ \tau_{xy}\end{pmatrix} = \begin{bmatrix}Q_{11} & Q_{12} & Q_{16}\\ Q_{12} & Q_{22} & Q_{26}\\ Q_{16} & Q_{26} & Q_{66}\end{bmatrix}\begin{pmatrix}\epsilon_{xx}\\ \epsilon_{yy}\\ \gamma_{xy}\end{pmatrix} \tag{5}$$

and

$$\tau_{xz}^{c} = G_{xz}^{c}\gamma_{xz}^{c}, \qquad \tau_{yz}^{c} = G_{yz}^{c}\gamma_{yz}^{c} \tag{6}$$

respectively; where the matrix composed of Q_{ij} is the transformed reduced stiffness matrix in the plane stress condition.

The Rayleigh–Ritz method is then applied to express the displacement field in a series of beam functions, $\zeta_i(x)$ and $\eta_i(y)$, in the x and y directions, respectively,

$$w(x,y,z,t) = \sum_{ij}\alpha_{ij}(t)\zeta_i(x)\eta_j(y)$$

$$\psi_x(x,y,z,t) = \sum_{ij}\beta_{ij}(t)\zeta_i'(x)\eta_j(y) \tag{7}$$

$$\psi_y(x,y,z,t) = \sum_{ij}\gamma_{ij}(t)\zeta_i(x)\eta_j'(y)$$

where $\zeta_i'(x)$ and $\eta_j'(y)$ are used to avoid the shear locking phenomenon when the sandwich panel becomes very thin. The form of the beam functions depends on the geometry and boundary conditions of the panels. A detailed description of the use of the beam function method can be found in Ref. 21.

To obtain the governing equations, the Hamilton principle is employed. Thus, the kinetic energy is expressed as

$$T = \frac{1}{2}\int_{-b}^{b}\int_{-a}^{a}\int_{h/2}^{(h/2)+t_f} 2\rho_f(\dot{u}^2+\dot{v}^2+\dot{w}^2)\,dz\,dx\,dy$$
$$+\frac{1}{2}\int_{-b}^{b}\int_{-a}^{a}\int_{-h/2}^{h/2}\rho_c\left(\dot{u}_c^2+\dot{v}_c^2+\dot{w}^2\right)dz\,dx\,dy \tag{8}$$

where ρ_f and ρ_c are the density of the face plates and the core, respectively. The strain energy becomes

$$V = \frac{1}{2}\int_{-b}^{b}\int_{-a}^{a}\int_{h/2}^{(h/2)+t_f} 2(\sigma_{xx}\epsilon_{xx}+\sigma_{yy}\epsilon_{yy}+\tau_{xy}\epsilon_{xy})\,dz\,dx\,dy$$
$$+\frac{1}{2}\int_{-b}^{b}\int_{-a}^{a}\int_{-h/2}^{h/2}\left(\tau_{xz}^{c}\epsilon_{xz}^{c}+\tau_{yz}^{c}\epsilon_{yz}^{c}\right)dz\,dx\,dy \tag{9}$$

Considering a point load $P(t)$ applied transversely on the panel at (x_0, y_0), the external work reads

$$W = \int_0^b\int_0^a P(t)\delta(x-x_0)\delta(y-y_0)w\,dx\,dy$$
$$= P(t)w(x_0,y_0) \tag{10}$$

Thus, the governing equations expressed in the generalized coordinates $\{q\}$ become

$$[M]\{\ddot{q}\} + [K]\{q\} = \{P^*\} \tag{11}$$

In this system of equations, $[M]$ and $[K]$ are $3N_1N_2 \times 3N_1N_2$ matrices, where N_1 and N_2 are the number of beam functions in the x and y directions, respectively, and $\{q\}$ and $\{P^*\}$ are vectors with $3N_1N_2$ dimension. The explicit form of the generalized coordinates is

$$\{q\}^T = \{\alpha_{11},\alpha_{12},\ldots,\alpha_{21},\ldots;\beta_{11},\beta_{12},\ldots,\beta_{21},\ldots;$$
$$\gamma_{11},\gamma_{12},\ldots,\gamma_{21},\ldots\}$$
$$= \{\{\alpha\}^T;\{\beta\}^T;\{\gamma\}^T\} \tag{12}$$

The generalized force P^* is obtained by substituting Eq. (7) into Eq. (10), i.e.,

$$W = P(t)\{q_1\}^T\{Y\} = \{q_1\}^T\{P^*\} \tag{13}$$

where

$$\{Y\}^T = \{\xi_1\eta_1,\xi_1\eta_2,\ldots,\xi_2\eta_1,\xi_2\eta_2,\ldots;0,\ldots;0,\ldots\} \tag{14}$$

$$\{q_1\}^T = \{\alpha_{11},\alpha_{12},\ldots,\alpha_{21},\ldots,0,\ldots,0,\ldots\} \tag{15}$$

Solution Procedure

In a forward analysis, Eq. (11) can be solved directly using such methods as the Newmark direct integration scheme.[22] Because the equations are coupled, however, the responses at any interesting locations, such as where the strain gauges are mounted, due to the external force applied at an arbitrary instant of time, are dependent on the responses at other locations of the structure. As a result, the responses of the whole structure need to be known to inversely determine the impact force, and this is considered infeasible. Thus, Eq. (11) is further manipulated for the purpose of inverse analysis.

Green's Function

Because the vibration modes of a structure with simple boundary conditions, such as simple supports, fixed ends, free ends, and supports with elastic springs, are orthogonal, transformation of the system of governing equations [Eq. (11)] to a coordinate that is expressed in terms of the vibration modes, i.e., to the eigenspace of the system of these second-order ordinary differential equations, can result in decoupled differential equations. Therefore, the right-hand side of Eq. (11) is set to be zero, and the natural frequencies and the vibration modes of the mathematical model can be obtained in a straightforward manner. Thus, the generalized coordinates, shown in Eq. (12), can be expressed as

$$\{q\} = \sum_{j=1}^{3N} a_j\{e_j\} = [X]\{a\} \tag{16}$$

where $[X]$ is the matrix formed by the vibration modes, i.e., the eigenvectors of the model formed by the beam functions shown in

Eq. (7). By the orthogonality characteristics of the eigenvectors, the system of governing equations is changed to

$$m_j\ddot{a}_j + k_j a_j = P(t)\left[\{e_j\}^T\{Y\}\right], \qquad j = 1, \ldots, 3N \tag{17}$$

where

$$m_j = \{e_j\}^T[M]\{e_j\}, \qquad k_j = m_j\omega_j^2 \tag{18}$$

Note that the $3N$ equations in Eq. (17) are decoupled and that each one can easily be solved by using the Laplace transform method. The solution in the form of the convolutional integral is

$$a_j(t) = \frac{\{e_j\}^T\{Y\}}{m_j\omega_j}\int_o^t P(\tau)\sin[\omega_j(t-\tau)]\,\mathrm{d}\tau \qquad j = 1, \ldots, 3N \tag{19}$$

By linearizing the impact force in each time step, Eq. (19) can be expressed in the following discrete form at $t = t_k$:

$$a_{j(k)} = \left(\{e_j\}^T\{Y\}\right)\left[\sum_{i=1}^{k-1} R(k-i, j)P_i + T(j)P_k\right] \tag{20}$$

where

$$R(l, j) = \frac{1}{k_j\omega_j\Delta t}\left[-\sin(\omega_j t_{l-1}) + 2\sin(\omega_j t_l) - \sin(\omega_j t_{l+1})\right] \tag{21}$$

$$T(j) = \frac{1}{k_j}\left[1 - \frac{\sin(\omega_j\Delta t)}{\omega_j\Delta t}\right]$$

For rigid-body modes, i.e., $w_j = 0$, Eqs. (21) can be changed to

$$R(l, j) = \frac{l(\Delta t)^2}{m_j}, \qquad T(j) = \frac{(\Delta t)^2}{6m_j} \tag{22}$$

Thus, the values of q, at any time instant t_k, can take the form

$$\{q\}_k = [X]\left(\sum_{i=1}^{k-1}[R][X]^T\{Y\}P_j[T][X]^T\{Y\}P_k\right) \tag{23}$$

and can be further arranged into

$$\{q\}_k = \sum_{n=1}^{k}\{Pg\}_{k+1-n}P_n \tag{24}$$

where

$$\{Pg\}_1 = [X][T][X]^T\{Y\}, \qquad \{Pg\}_{n+1} = [X][R][X]^T\{Y\} \qquad 1 \le n \le k-1 \tag{25}$$

Further, $\{Pg\}$ can be decomposed into the following three portions, which are consistent with the form shown in Eq. (12):

$$\{Pg\}^T = \left\{\{Pg_1\}^T, \{Pg_2\}^T, \{Pg_3\}^T\right\} \tag{26}$$

By substituting Eq. (24) into Eqs. (1), (2), and (7), the response of the sandwich panel in terms of the displacement variables can be directly obtained. Because in this study the responses were recorded using strain gauges mounted on the surfaces of the face plates, the force-vs-strain relationship can be written as

$$\epsilon^{(k)} = \sum_{n=1}^{k} G_{k+1-n}P_n \tag{27}$$

where G is Green's function matrix. The explicit form of Green's functions in the x and y directions on the upper and lower face plates is

$$G_x = \{\Gamma_1\}^T\{Pg_2\} + \{\Gamma_2\}^T\{Pg_1\}$$
$$G_y = \{\Gamma_3\}^T\{Pg_3\} + \{\Gamma_4\}^T\{Pg_1\} \tag{28}$$

where

$$\{\Gamma_1\} = \mp\tfrac{1}{2}(h+t)\{\zeta_1''\eta_1, \zeta_1''\eta_2, \ldots, \zeta_1''\eta_{N2}, \zeta_2''\eta_1, \ldots, \zeta_{N1}''\eta_{N2}\}$$
$$\{\Gamma_2\} = -[z \mp (h+t)/2] \times \{\zeta_1''\eta_1, \zeta_1''\eta_2, \ldots, \zeta_1''\eta_{N2}, \zeta_2''\eta_1, \ldots, \zeta_{N1}''\eta_{N2}\} \tag{29}$$
$$\{\Gamma_3\} = \mp\tfrac{1}{2}(h+t)\{\zeta_1\eta_1'', \zeta_1\eta_2'', \ldots, \zeta_1\eta_{N2}'', \zeta_2\eta_1'', \ldots, \zeta_{N1}\eta_{N2}''\}$$
$$\{\Gamma_4\} = -[z \mp (h+t)/2]\{\zeta_1\eta_1'', \zeta_1\eta_2'', \ldots, \zeta_1\eta_{N2}'', \zeta_2\eta_1'', \ldots, \zeta_{N1}\eta_{N2}''\}$$

where the $-$ sign and $+$ sign in the $\mp$ symbol are for the upper and lower face plates, respectively.

Algorithms for Forward and Inverse Analyses

If the whole duration of interest in an impact event is divided into n time steps, then Eq. (27) becomes

$$\begin{pmatrix} r_1 \\ r_2 \\ r_3 \\ \vdots \\ r_n \end{pmatrix} = \begin{bmatrix} G_1 & & & & \\ G_2 & G_1 & & & \\ G_3 & G_2 & G_1 & & \\ \vdots & \vdots & \vdots & \ddots & \\ G_n & G_{n-1} & G_{n-2} & \ldots & G_1 \end{bmatrix}\begin{pmatrix} P_1 \\ P_2 \\ P_3 \\ \vdots \\ P_n \end{pmatrix} \tag{30}$$

In Eqs. (30), all of the off-diagonal terms in the upper-right-hand portion of Green's function matrix are equal to zero, i.e.,

$$G(i, j) = \begin{cases} 0 & \text{if} \quad j > i \\ G_{i+1-j} & \text{if} \quad i \ge j \end{cases} \tag{31}$$

This satisfies the causality law.

In the forward analysis, the impact force is known, and the responses of the panel are to be determined. Thus, Eq. (30) can be solved directly.

In the inverse analysis, on the other hand, the impact force is to be extracted from the recorded responses of the panel. Past experience has shown that a direct solution procedure using schemes such as Gauss elimination always gives divergent results for the obtained impact force.[21,23–27] This is because Eq. (30) is ill posed, and noises are always embedded in the recorded response data. Meanwhile, deviation always exists between the developed mathematical model and the actual structure to be struck. This deviation may result from the imperfection of the structure used as the target and the limitation in formulation of Green's function. Note that Green's function was constructed based on assumptions such as the simplified displacement field, homogenization of the honeycomb core, a finite number of eigenvectors, etc.

Therefore, one can only expect to extract an optimal impact force history from the recorded noise-contaminated strain data by means of the decoupled derived Green's function. Thus, an optimization scheme is employed to search for the impact force history from the recorded response data. When there exists more than one sensor to record the response data, for ease of explanation, Eq. (30) is further expressed as

$$\boldsymbol{r}_{(j)} = \boldsymbol{G}_{(j)}\boldsymbol{P}, \qquad \boldsymbol{N} \ge \boldsymbol{j} \ge \boldsymbol{1} \tag{32}$$

where $\boldsymbol{N}$ is the number of sensors used in an impact event. Then an objective function is constructed as follows:

$$\boldsymbol{E} = \sum_{j=1}^{N}\left(\boldsymbol{r}_{(j)} - \boldsymbol{G}_{(j)}\boldsymbol{P}\right)^T\left(\boldsymbol{r}_{(j)} - \boldsymbol{G}_{(j)}\boldsymbol{P}\right) \tag{33}$$

Thus, the problem of solving Eq. (32) is converted to searching for the optimal impact force $\boldsymbol{P}$ in Eq. (33) such that the value of the objective function $\boldsymbol{E}$ becomes minimal. Because Eq. (33) is in a quadratic form in $\boldsymbol{G}$ and $\boldsymbol{G}^T\boldsymbol{G}$ is semidefinite, the searched optimal force $\boldsymbol{P}$ must be such that $\boldsymbol{E}$ is of the global minimal value. Further, because the impact force history is never in tension, the following

physical constraint can be imposed to further enhance the quality of the searched impact force:

$$\boldsymbol{P} \geq 0 \tag{34}$$

Therefore, the problem of solving for the impact force history becomes a constrained optimization problem. In this study, the gradient projection method is employed,[28] and the search procedure continues until the difference in the values of the objective function in the last 10 search steps becomes smaller than a preset value. The details of setting up the convergent criterion for use in the search process can be found in Ref. 21.

Experimental Procedure

Specimen Preparation

The face plates of the specimen were fabricated from 1076E Fiberite T300/976 graphite/epoxy prepregs. The stacking sequence was always $[0/45/90/-45]_{2S}$. Although the developed model can be applied to sandwich panels having various types of core,[22] in this study Hexcel CRIII-3.175-5052-0.0381-97.909-10.0 honeycomb was selected.[29,30] The numbers shown in the Hexcel specification are the cell size, aluminum type, thickness of the honeycomb wall, density, and height of the core. The honeycomb was made of 5052-H39 aluminum. Use of the honeycomb core aimed at investigating the versatility of the developed displacement field because honeycomb is inhomogeneous and anisotropic. The adhesive used was Cyanamid epoxy Type FM300K with a thickness of 0.1 mm. To fabricate the sandwich panel, the face plates, adhesive, and honeycomb were cut into 302 × 302 mm pieces, as shown in Fig. 2, and were cured in an autoclave according to the manufacturer's fabrication procedure. The total thickness of the specimen was 14 mm, in which the adhesive was found to make a negligible contribution to the total thickness of the specimen after the curing process.

The material properties of the graphite/epoxy face plates were[24]

$$E_1 = 121.6 \text{ GPa}, \qquad E_2 = E_3 = 9.17 \text{ GPa}$$

$$G_{12} = G_{13} = 5.21 \text{ GPa}, \qquad G_{23} = 3.22 \text{ GPa} \tag{35}$$

$$\nu_{12} = \nu_{13} = 0.29, \qquad \nu_{23} = 0.42, \qquad \rho = 1553 \text{ kg/m}^3$$

The transverse shear modulus, based on the formula proposed by Gibson and Ashby,[31] is $G^c_{xz} = G^c_{yz} = 0.312$ GPa. The weight of the adhesive was smeared into the honeycomb, and the averaged density of the honeycomb/adhesive became $\rho' = 177.71$ kg/m^3.

Experimental Setup

To avoid the effect of boundary imperfection occurring under either the clamped or the simply supported boundary conditions, a free support condition was used during the impact test. Thus, the sandwich panel was suspended by two light strings. Three Kyowa KFG-2-350-C1-11 strain gauges were mounted on the impact side of the face plate. The locations were (30, 0, 7), (80, 0, 7), and (0, 70, 7) mm, for the G1, G2, and G3 gauges, respectively, as shown in Fig. 2. Note that the origin of the coordinate system was at the panel center. The strain data were amplified by Kyowa CDV230C signal conditioners, whose frequency response was as high as 200 kHz. Impact was conducted using a PCB 086B04 instrumented hammer with a sensitivity of 10.9 mV/N. The tip of the hammer was 3 mm in diameter. Thus, the impact force was approximated as a point load. The tip of the hammer was marked by chalk to trace the striking location on the face plate of the panel during impact. All of the signals, including both the force and the strains, were recorded using a Nicolet 440 digital storage oscilloscope. The sampling rate was set to 1 μs.

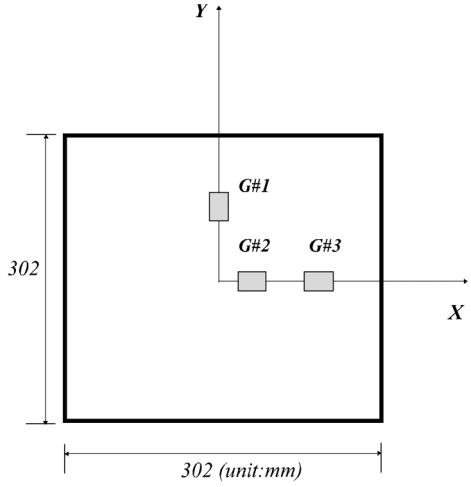

Fig. 2 Dimensions and coordinates of the sandwich panel. Three gauges were mounted on the impact side of the face plates; coordinates in millimeters were (30, 0, 7), (80, 0, 7), and (0, 70, 7) for gauges 1, 2, and 3, respectively.

Verification and Discussion

In all of the forward and inverse analyses, the number of modes used to construct Green's function was 100, i.e., 10 beam functions in both x and y directions. The frequency corresponding to the highest mode was higher than 100 kHz. This frequency was considered to be high enough because the frequency band of the impact force induced by the instrumented hammer was usually from dc to 20 kHz (Ref. 25). Numerical runs were also conducted using 225 modes to construct Green's function, and the deviation of the predictions using 100 and 225 modes was found to be negligible.[22] Because the deviation between the prediction using a 2-μs time step and that using a 1-μs time step has been found to be negligible,[22] all of the analytical results shown were obtained using a 2-μs time step in the analysis.

Forward Analysis

Responses in Far Fields

Figure 3 shows the force history from a typical impact event. The impact location was at (−2, −101, 7) mm using the coordinates plotted in Fig. 2. The distances between the impact location and the locations of the three strain gauges were 106, 130, and 171 mm, which corresponded to panel thickness ratios of 7.6, 9.3, and 12.2, respectively. The duration of impact was approximately 880 μs. Because the peak impact force was small, there should have been no damage to the panel after impact.[32] The recorded strain responses and the predictions using the method described in preceding sections along with the impact force shown in Fig. 3 are all plotted in Figs. 4a–4c. The agreement is considered to be satisfactory. Other similar comparison results, including those of the sandwich panels whose face plates were made from aluminum sheets, can be found in the examples shown in Ref. 22. Because the distances between the strains recorded and the impact location were several times greater than the panel thickness, the local effect of the responses occurred in the impact neighborhood at the very beginning stage where impact has died out. Thus, the model presented is considered

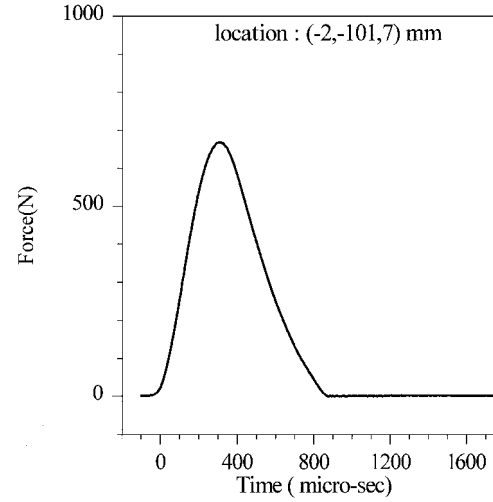

Fig. 3 Impact force exerted by an instrumented hammer at a coordinate (− 2, − 101, 7) mm on the sandwich panel.

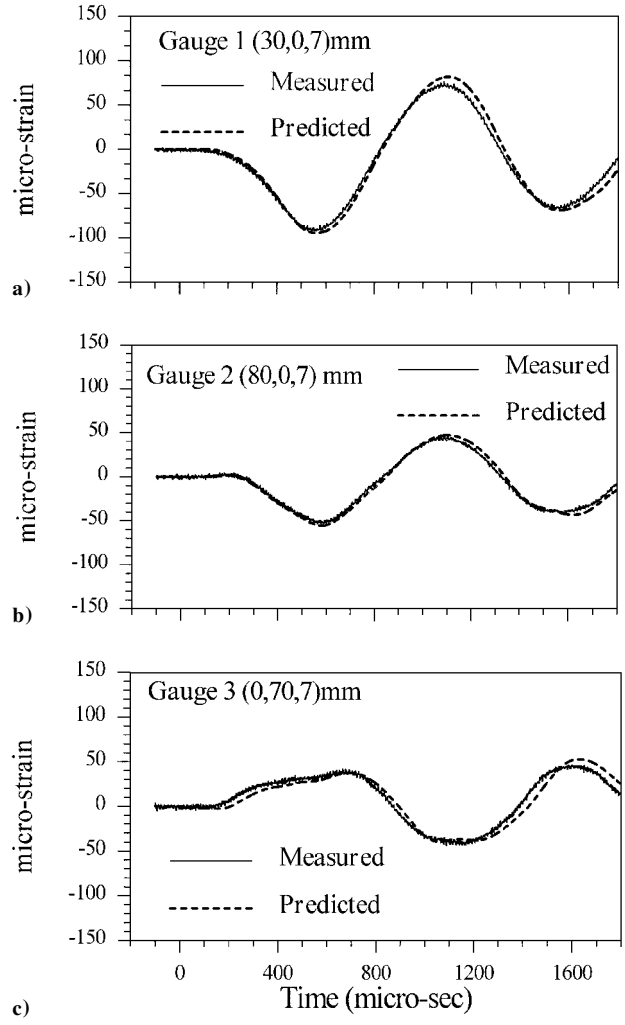

Fig. 4 Measured and predicted strain histories, where distances between the gauges and the impact point were 10.6, 13.0, and 17.1, respectively, times the panel thickness, by the applied impact force plotted in Fig. 3.

to be suitable for predicting far-field responses of sandwich panels with honeycomb core under low-velocity impact conditions. On the other hand, the commonly used displacement theories for laminated plates, such as the first-order shear deformation theory and the classical lamination theory, were found to result in a significant deviation for sandwich panels under both quasistatic and dynamic loading conditions.[22,33]

Responses in Near Fields

To investigate the effect of the distances between the striking and the strain gauge locations, another impact run was conducted. The impact force is plotted in Fig. 5, and the corresponding recorded responses are shown in Figs. 6a–6c. In this test run, the impact location was at (3, 1, 7) mm. The distances between the location of impact and the locations of the gauges were 27, 77, and 69 mm, which were 1.9, 5.5, and 4.9 times the panel thickness, respectively. Also plotted in Figs. 6a–6c are the predictions of the forward analyses. It is found from this comparison that, although the agreement between the predicted and the measured results shown in Figs. 6b and 6c is generally satisfactory, as expected the deviation in Fig. 6a is more significant at the beginning stage of impact. This more significant deviation is considered to be due to neglect in the model of the transverse normal deformation and the local heterogeneity characteristics of the honeycomb core. Both of these mechanisms were considered to affect the response of the panel only in the local region of impact and within a very short time period. As the impact process continued, the sandwich panel was gradually governed by the global motion instead of the local disturbance. Thus, the agreement between the predictions and the measured data became

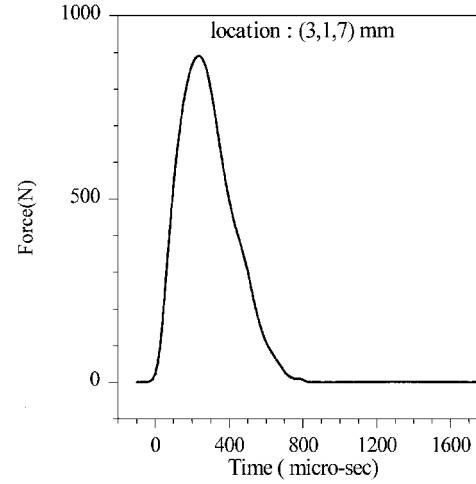

Fig. 5 Impact force exerted by an instrumented hammer at a coordinate (3, 1, 7) mm on the sandwich panel.

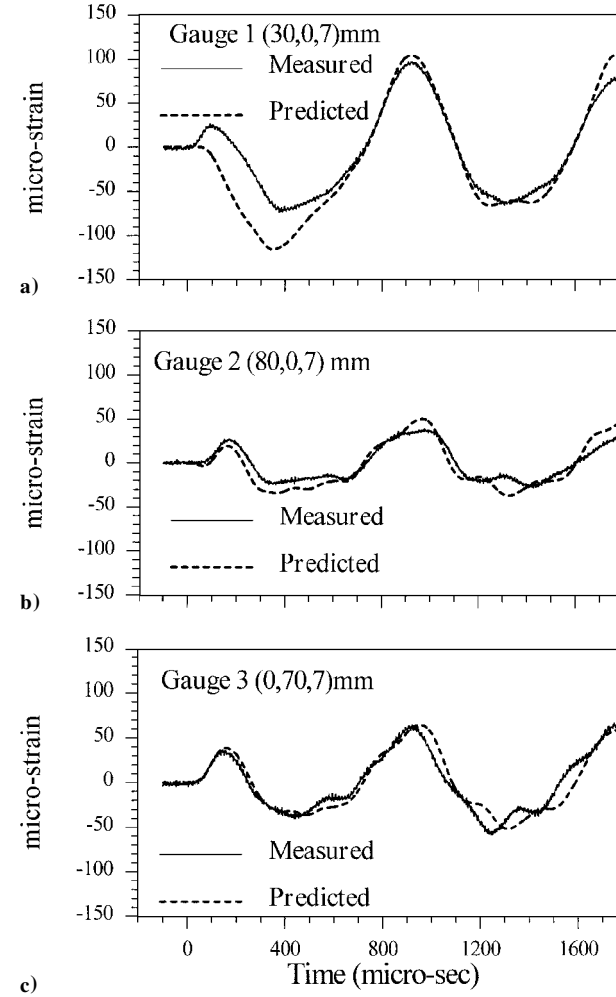

Fig. 6 Measured and predicted strain histories, where distances between the gauges and the impact point were 1.9, 5.5, and 4.9, respectively, times the panel thickness, by the applied impact force plotted in Fig. 5.

generally more satisfactory, as is also demonstrated in Fig. 6a at a period approximately 600 μs after the onset of impact. Additional work is underway to construct another refined mathematical model that accommodates this local and highly transient behavior of the sandwich panel under low-velocity impact conditions.

Inverse Analysis

As described in a preceding section, to perform inverse analysis is to extract impact force from the corresponding response data. For

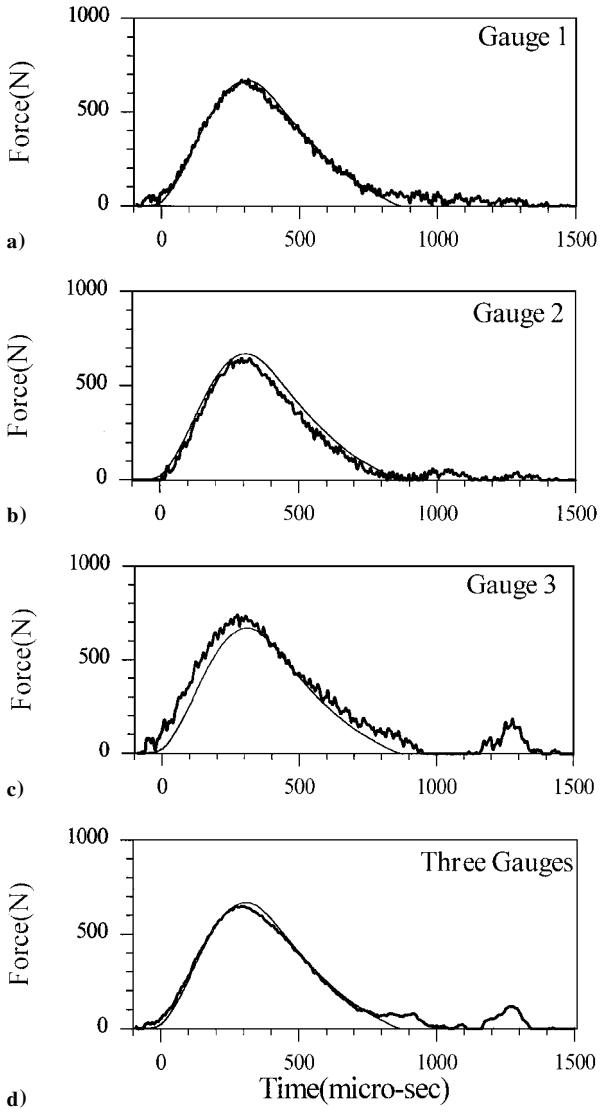

Fig. 7 Recorded (——) and identified (——) impact forces obtained using the strains recorded by the indicated gauges as the input data in the inverse analyses. (This impact event is the same as that with results shown in Figs. 3 and 4.)

illustration purposes, the impact test run identical to that with results shown in Figs. 3 and 4 was employed. Thus, the measured strains in Fig. 4 were used as the known data. The determined impact force histories are plotted in Figs. 7a–7c using the responses recorded by gauges G1–G3, respectively. That is, N was set to 1 in Eq. (33). The agreement is considered to be very satisfactory, especially for the runs in which gauges G1 and G2 were used as the input data. On the other hand, the deviation between the prediction and the result shown in Fig. 7c is slightly larger, and there also exists a more significant deviation between the prediction and the data at the beginning stage of impact, as shown in Fig. 4c. This is because the response of the panel at the beginning stage of impact has a more significant influence on the entire history of the determined impact force, as can also be observed from Eq. (30) and the optimization algorithm. Thus, an accurate model is essential to obtain satisfactory agreement in both the forward and the inverse analyses. On the other hand, it is observed that the deviation between the determined and measured impact force at the ending stage of impact was generally larger. This is because the force at this time stage only affected the response in an even later time period of the impact run. As a result, its weighting was much smaller, and the force in this region was more difficult to accurately determine in the optimization process.

The effect of using the data recorded by all three gauges to determine the impact force history is shown in the result plotted in Fig. 7d. In this run, N was set to be 3 in Eq. (33). Because the results recorded from multiple gauges were used, the effect of noise was suppressed. As a result, the determined force has a smoother profile. The general agreement between the determined and the recorded force data is also considered to be more satisfactory than the agreement found in Figs. 7a–7c using the responses recorded by a single gauge, although a small erroneous force peak still exists at the very end of the impact event.

Conclusions

A Green's function method, which was constructed on the basis of a feasible analytical model, has been presented for forward and inverse analyses of impact on a sandwich panel. The face plates of the panel were made of graphite/epoxy composite laminates, and the core was made of honeycombs. The displacement field of the panel was modeled by considering the transverse shear deformation of the core and both the membrane and the bending deformations of the face plates. This displacement field was then expressed in a generalized coordinate formed by means of a series of beam functions. The coupled equations of motion were then constructed using the Hamilton principle to model the response of the panel in an impact event. To construct Green's function, which is needed in the inverse analysis, the coupled equations of motion have been further transferred to the eigenspace to obtain the convolution relationship in a decoupled form, and a constrained optimization algorithm has been employed to search for the impact force history from the recorded response data.

In the forward analyses, the use of the model has resulted in a very satisfactory correlation with the recorded data when the distances between the impact point and the gauges were a few times the thickness of the panel. As the distances between the striking and the gauge locations decreased, the deviation was found to be more significant at the beginning stage of impact. This is considered to be due to neglect in the constructed model of the transverse normal deformation and local heterogeneity of the honeycomb core, which affect only the highly transient response of the panel in the neighborhood of the impact location. On the other hand, the developed inverse analysis method was found to provide a very good correlation between the measured and the detected impact force. The use of data recorded by multiple gauges to determine the impact force was found to provide better overall correlation with the measured force than the use of the data from a single gauge did. Thus, this forward and inverse analysis method is considered to be suitable for predicting the impact response as well as for determining the impact force history of a sandwich panel under low-velocity impact conditions. Further, this Green's function approach is considered to be generally applicable to forward and inverse analyses of other types of structures subjected to low-velocity impact as long as the governing equation, i.e., Eq. (11), is properly constructed.

Acknowledgments

This work was supported by the National Science Council of Taiwan, Republic of China, under Contracts NSC 84-2623-D-002-013 and NSC 85-2212-E-002-042. Supply of honeycomb materials and laminated plates by the Chung-Shan Institute of Science and Technology of the Republic of China is gratefully acknowledged.

References

[1]Reissner, E., "Finite Deflections of Sandwich Plates," *Journal of the Aeronautical Sciences*, Vol. 15, 1948, pp. 435–440.

[2]Hoff, N. J., and Mautner, S. E., "Bending and Buckling of Sandwich Beams," *Journal of the Aeronautical Sciences*, Vol. 15, 1948, pp. 707–720.

[3]Plantema, F. J., *Sandwich Construction*, Wiley, New York, 1966.

[4]Allen, H. G., *Analysis and Design of Structural Sandwich Panels*, Pergamon, Oxford, England, UK, 1969.

[5]Yu, Y. Y., "A New Theory of Elastic Sandwich Plates: One-Dimensional Case," *Journal of Applied Mechanics*, Vol. 26, 1959, pp. 415–421.

[6]Yu, Y. Y., "Simple Thickness-Shear Modes of Vibration of Infinite Sandwich Plates," *Journal of Applied Mechanics*, Vol. 26, 1959, pp. 679–681.

[7]Yu, Y. Y., "Flexural Vibrations of Elastic Sandwich Plates," *Journal of the Aeronautical Sciences*, Vol. 27, 1960, pp. 272–282.

[8]Yu, Y. Y., "Simplified Vibrations of Elastic Sandwich Plates," *Journal of the Aeronautical Sciences*, Vol. 27, 1960, pp. 894–900.

[9]Folie, G. M., "Bending of Clamped Orthotropic Sandwich Plates," *Journal of Engineering Mechanics*, Vol. 96, 1970, pp. 243–265.

[10]Kanematsu, H. H., Hirano, Y., and Iyama, H., "Bending and Vibration of CFRP-Faced Rectangular Sandwich Plates," *Composite Structures*, Vol. 10, 1988, pp. 145–163.

[11]Khatua, T. P., and Cheung, Y. K., "Bending and Vibration of Multi-Layer Sandwich Beams and Plates," *International Journal for Numerical Methods in Engineering*, Vol. 6, 1973, pp. 11–24.

[12]Chang, J. S., and Chen, H. C., "Free Vibration of Sandwich Plate with Variable Thickness," *Journal of Sound and Vibration*, Vol. 155, No. 2, 1992, pp. 195–208.

[13]Sun, C. T., and Wu, C. T., "Low Velocity Impact of Composite Sandwich Panels," AIAA Paper 91-1077, 1991.

[14]Lee, L. J., Huang, K. J., and Fann, Y. J., "Dynamic Responses of Composite Sandwich Plate Impacted by a Rigid Ball," *Journal of Composite Materials*, Vol. 27, 1993, pp. 1238–1256.

[15]Abrate, S., "Localized Impact on Sandwich Structures with Laminated Facings," *Applied Mechanics Review*, Vol. 50, No. 2, 1997, pp. 69–82.

[16]Goldsmith, W., and Sackman, J. L., "An Experimental Study of Energy Absorption in Impact on Sandwich Plates," *International Journal of Impact Engineering*, Vol. 12, 1992, pp. 241–262.

[17]Mines, R. A. W., Worrall, C. M., and Gibson, A. G., "The Static and Impact Behaviour of Polymer Composite Sandwich Beams," *Composites*, Vol. 25, 1994, pp. 95–110.

[18]Wu, E., and Jiang, W. S., "Axial Crush of Metallic Honeycombs," *International Journal of Impact Engineering*, Vol. 18, 1997, pp. 439–456.

[19]Martin, M. T., and Doyle, J. F., "Impact Force Identification from Wave Propagation Responses," *International Journal of Impact Engineering*, Vol. 18, No. 1, 1996, pp. 65–77.

[20]Doyle, J. F., "Experimentally Determining the Contact Force During the Transverse Impact of an Orthotropic Plate," *Journal of Sound and Vibration*, Vol. 118, No. 3, 1987, pp. 441–448.

[21]Wu, E., Yeh, J. C., and Yen, C. S., "Impact on Composite Laminated Plates: An Inverse Method," *International Journal of Impact Engineering*, Vol. 15, 1994, pp. 417–433.

[22]Luo, B. H., "An Analytical and Experimental Study of Sandwich Structures Under Low-Velocity Impact Conditions," M.S. Thesis, Inst. of Applied Mechanics, National Taiwan Univ., Taiwan, ROC, 1996.

[23]Inoue, H., Kishimoto, K., Shibuya, T., and Koizumi, T., "Estimation of Impact Load by Inverse Analysis," *Japan Society of Mechanical Engineers, International Journal*, Series I, Vol. 35, 1992, pp. 420–427.

[24]Yen, C. S., and Wu, E., "On the Inverse Problems of Rectangular Plates Subjected to Elastic Impact, Part 1: Method Development and Numerical Verification," *Journal of Applied Mechanics*, Vol. 62, 1995, pp. 692–698.

[25]Yen, C. S., and Wu, E., "On the Inverse Problems of Rectangular Plates Subjected to Elastic Impact, Part 2: Experimental Verification and Further Applications," *Journal of Applied Mechanics*, Vol. 62, 1995, pp. 699–705.

[26]Wu, E., Yeh, J. C., and Yen, C. S., "Identification of Impact Forces at Multiple Locations on Laminated Plates," *AIAA Journal*, Vol. 34, 1994, pp. 2433–2439.

[27]Wu, E., Tsai, T. D., and Yen, C. S., "Two Methods for Determining Impact Force History on Elastic Plates," *Experimental Mechanics*, Vol. 35, 1995, pp. 11–18.

[28]Arora, J. S., *Introduction to Optimum Design*, McGraw–Hill, New York, 1989.

[29]"Mechanical Properties of Hexcel Honeycomb Material," Hexcel Corp., TSB120, 1986.

[30]"The Basics on Bonded Sandwich Construction," Hexcel Corp., TSB 124, 1987.

[31]Gibson, L. J., and Ashby, F. M., *Cellular Solids, Structure and Properties*, Pergamon, Oxford, England, UK, 1988.

[32]Wu, E., and Shyu, K., "Response of Composite Laminates to Contact Loads and Relationship to Low-Velocity Impact," *Journal of Composite Materials*, Vol. 27, 1993, pp. 1443–1464.

[33]Chen, H. C., "Experimental and Numerical Study of Free Vibration for Sandwich Panels with Variable Thickness," Ph.D. Dissertation, Inst. of Applied Mechanics, National Taiwan Univ., Taiwan, ROC, 1992.

R. K. Kapania
Associate Editor